

## Title

# The Earth as a benchmark: spectropolarimetry unveils strong bio-signatures

## Authors

Michael F. Sterzik, European Southern Observatory, Santiago, Chile

Stefano Bagnulo, Armagh Observatory, Armagh, Northern Ireland, U.K.

Enric Pallé, Instituto de Astrofísica de Canarias, Tenerife, Spain

## Text

*Low-resolution intensity spectra of the Earth's atmosphere obtained from space reveal strong bio-signatures such as molecular oxygen and methane with abundances far from chemical equilibrium, as well as the presence of a 'red edge' caused by surface vegetation<sup>1</sup>. In the Earth's atmosphere, light is also strongly linearly polarized by scattering by air molecules, aerosols and cloud particles, and by reflection from oceans and land<sup>2</sup>.*

*Spectropolarimetric observations of local patches of Earth's skylight contain signatures of oxygen, ozone and water, and are used to characterize the properties of clouds and aerosols<sup>3,4</sup>. Applied to exoplanets, ground-based spectropolarimetry has advantages to better constrain atmospheres and surfaces than standard intensity spectroscopy<sup>5-9</sup>.*

*Here we report disk-integrated linear polarization spectra of the Earth as seen from space. The spectra are obtained by observations of the Earthshine, which is sunlight that has been first reflected by the Earth and then reflected back to Earth by the Moon<sup>10-13</sup>. These observations allow us to determine the fractional contribution of clouds and ocean surface, and are sensitive to*

***visible areas of vegetation as small as 10%. They represent a benchmark for the diagnostics of the atmospheric composition, mean cloud height, and surfaces of exosolar planets.***

Broadband polarimetric measurements of the disk-integrated Earth have been obtained previously<sup>14</sup>. Observations of the Earthshine at a wavelength of 550nm reported a fraction of linear polarization of about 10% for a phase angle near to 90°. Since the lunar surface is responsible for a depolarization of the incident light by a factor of  $\sim 3.3$ , the true linear polarization of the disk-integrated light of the Earth was estimated to be around 30-35%<sup>14</sup>. Modern estimates of the Earth's polarization are based on the satellite borne instrument POLDER in three bands (443nm, 670nm and 865nm) and demonstrate the strong dependence on cloud cover, and on wavelength<sup>15</sup>. These measurements, however, do not allow a spectral analysis, and therefore cannot be used to infer bio-signatures.

Using the FOcal Reducer/low-dispersion Spectrograph FORS<sup>16</sup> mounted at the Very Large Telescope in Chile, we measured the linear polarization spectra of the Earthshine. Our **data were collected during two observing epochs** near quadrature, with distinct viewing geometries of the Earth (the observing techniques and data reduction details are given in the Supplementary Information). A detailed breakdown of the surfaces visible in our Earthshine observations, derived from MODIS satellite observations<sup>17</sup>, is given in Table 1.

The red curves in the Figures display the fraction of linear polarization  $P_Q(\lambda)$  (=  $Q/I$ , the polarized flux  $Q$  over the total flux  $I$ ) measured in April (Fig. 1) and in

June (Fig. 2). The shape of the  $P_Q(\lambda)$  profile depends mainly on the Earth's surface albedo at the time of observations. In April, the continuum polarization reaches about 9% at 500nm, and decreases smoothly to 4% at 900nm. The polarization observed in June is 3% higher than observed in April. A change of the continuum slope occurs visibly in the June spectrum at a wavelength of around 520nm. In particular the June spectrum matches Dollfus<sup>14</sup> observation of 10% Earthshine polarization at his observing wavelength of 550nm, while our April value is smaller. In order to display the detailed structure on top of the smooth continuum, we have fit and subtracted from the observed  $P_Q(\lambda)$  profile a fourth-order polynomial (between 530 and 910nm). The residual signal  $\delta P(\lambda)$  shows a rich structure at the 0.1% level. A narrow O<sub>2</sub>-A band is prominent in both spectra at the level of almost 1% above the continuum. O<sub>2</sub>-B (690nm) and H<sub>2</sub>O (720 and 820nm) bands are broader and with lower amplitude. An additional (strong) polarization feature is present in the June spectrum close to 850nm, and a (weak) feature at 854nm. We tentatively attribute it due to the presence of a variable, thin CaII layer in the Earth's ionosphere recently discovered through observations of the transmitted spectrum of the Earth<sup>18</sup>. Remarkably, the overall shape of the residuals between 550 and 750nm differs between the two epochs: while the April spectrum exhibits a broad, shallow peak around 700nm, the June spectrum appears rather flat.

We compared our measurements with the polarization estimated from POLDER data<sup>15</sup>, and with **published tables of** radiative transfer models of Earth-like extrasolar planets<sup>5</sup>. For comparison purposes, both POLDER data and model predictions have to be scaled to account for the depolarization of the Earthshine

caused by reflection on the lunar surface. The lunar depolarization factor is not well determined, but roughly correlates with the albedo of the reflecting surfaces<sup>19,20</sup>. Following a classic study, we assume a linear increase of depolarization with wavelength, normalized to 3.3 at a wavelength at 550nm<sup>14</sup> ( $= 3.3 \lambda[\text{nm}]/550$ ).

The interpretation of the POLDER data depends on the cloud coverage **at the time of observation** and is roughly consistent with our continuum values in April, but too low in June. The **higher** polarization we observed **in June** can be qualitatively explained by an approximately 20% **lower** cloud coverage during our Earthshine measurements than assumed for the disk-integration of the POLDER data<sup>15</sup>.

For the comparisons with theoretical predictions, we have constructed a fine grid of possible Earth spectra **from published tables** by varying the parameters in steps of 1% for the different scene types<sup>5</sup> (Ocean clouded/clear and Vegetation clouded/clear). Then we have compared these models with our observations in the wavelength region between 420nm and 530nm. In the blue spectral range, the impact of cloud properties on the polarization is minor<sup>19</sup> and synthetic Earth model polarized spectra agree quantitatively with our observations. The parameters of the best fitting models are listed in Table 2 (April “c” and June “c”). For both observing epochs, the modeling results match MODIS derived cloud coverage fractions calculated for clouds having optical depth  $\tau > 6$ . The June model - less affected by clouds - approximates the continuum well. However, the models<sup>5</sup> predict systematically polarizations in the

red part of the continuum that are too low, primarily because of the **approximations used in the models** for the cloud microphysics<sup>22</sup>. Real clouds **are patchy and**, in particular over the ocean, exhibit much larger mean effective radii (droplet sizes 12-15  $\mu\text{m}$ ) and a high variation in their optical depth distribution<sup>23</sup>. **Depending on the underlying surface types, higher polarization degrees are thus expected.**

Guided by the actual observed surface scene fractions (Table 1), we have calculated more polarization spectra **from tabulated model spectra**<sup>5</sup> with parameters that are other plausible approximations to the real surface fractions responsible for the Earthshine spectrum at the epoch of the observations (model class parameters “a” and “b”). While these models fail to explain the continuum, their residual profiles (generated with the same fourth-order polynomial fit and subtraction from the continuum as adopted as for the observed spectra) are consistent with our observations.

Indicated by horizontal lines, we have hatched two bandpass regions at 650-680nm and 740-800nm and calculated the normalized difference vegetation index (NDVI)<sup>24</sup>. A larger contrast in the continuum averages in April than in June is interpreted by the presence of a Vegetation Red Edge signal in April, which is practically undetected in June. The Vegetation Red Edge feature in the April spectra can be reproduced by assuming about 10-15% cloud-free land-vegetation (model April-a of Table 2). A smaller fraction (model April-b and April-c) reduces the NDVI contrast too much, while too large a fraction would overestimate the observed feature. Similarly, the June data can best be described

Spectropolarimetry unveils strong biosignatures

through little or absent cloud-free vegetation surfaces (model June-a and June-c), while a 10% cloud-free vegetation fraction produces a NDVI that is too pronounced to be compatible with the data (model June-b). We estimate that our data are sensitive to variations of 5% in the NDVI. Also the observed polarization peak of the O<sub>2</sub>-A feature (and to a lesser extent O<sub>2</sub>-B) is fully compatible with the models. The amplitude of these features are sensitive to the top of the cloud layer, and to the O<sub>2</sub> mixing ratio. Our Earthshine observations suggest a low top-layer (around 800hPa), **assuming the mixing ratio on Earth as fixed**<sup>5</sup>. Also the H<sub>2</sub>O and O<sub>3</sub> (580nm) band strengths appear fully consistent with the model.

**Our spectropolarimetric measurements of the Earthshine constrain the Earth's surface and atmospheric composition and bio-signatures. Improved vector radiative transfer models with more realistic cloud and surface treatment are necessary to fully account for the observed spectra. Validation of these models is necessary to interpret Earth-like exoplanet polarization spectra.**

## References

- 1: Sagan, C., Thompson, W.R., Carlson, R., Gurnett, D., Hord., C. A search for life on earth from the Galileo spacecraft. *Nature* 365, 715-721 (1993).
- 2: Coffeen, D.L. Polarization and scattering characteristics in the atmospheres of Earth, Venus, and Jupiter. *J. Opt. Soc. Am.*, Vol. 69., No. 8, 1051-1064 (1979).
- 3: Aben, I., Helderman, F., Stam, D.M., Stammes, P. Spectral fine-structure in the polarization of skylight. *Geophysical Research Letters*, Vol. 26, No. 5, 591-594 (1999).
- 4: Boesche, E., Stammes, P., Preusker, R., Bennartz, R., Knap, W., Fischer, J. Polarization of skylight in the O<sub>2</sub>A band: effects of aerosol properties. *Applied Optics*, Vol. 47, No. 19, 3467-3480 (2008).
- 5: Stam, D.M. Spectropolarimetric signatures of Earth-like extrasolar planets. *Astron. Astrophys.* 482, 989-1007 (2008).
- 6: Buenzli, E., Schmid, H.M. A grid of polarization models for Rayleigh scattering planetary atmospheres. *Astron. Astrophys.* 504, 259-276 (2009).
- 7: Keller, C.U. et al. EPOL: the exoplanet polarimeter for EPICS at the E-ELT. *Proc. of SPIE*, 7735, pp 77356G-77356G-13 (2010).

Spectropolarimetry unveils strong biosignatures

8: Bailey, J. Rainbows, Polarization, and the Search for Habitable Planets.

*Astrobiology* 7, 320-332 (2007).

9: Williams, D.M., Gaidos, E. Detecting the glint of starlight on the oceans of distant planets. *Icarus* 195, 927-937 (2008).

10: Arnold, L., Gillet, S., Lardiere, O., Riaud, P., Schneider, J. A test for the search for life on extrasolar planets. Looking for the terrestrial vegetation signature in the Earthshine spectrum. *Astron. Astrophys.* 392, 231-237 (2002).

11: Woolf, N.J., Smith, P.S., Traub, W.A., Jucks, K.W. The Spectrum of Earthshine: A Pale Blue Dot Observed from the Ground. *Astrophys. J.* 574, 430-433 (2002).

12: Seager, S., Turner, E.L., Schafer, J., Ford, E.B. Vegetation's Red Edge: A Possible Spectroscopic Biosignature of Extraterrestrial Plants. *Astrobiology* 5, 372-390 (2005).

13: Montanes-Rodriguez, P., Palle, E., Goode, P.R., Martin-Torres, F.J. 2006. Vegetation Signature in the Observed Globally Integrated Spectrum of Earth Considering Simultaneous Cloud Data: Applications for Extrasolar Planets. *The Astrophys. J.* 651, 544-552.

14: Dollfus, A. Etudes des planetes par la polarisation de leur luminiere. *Supplements aux Annales d' Astrophysique* 4, 58-70 (1957).



- 15: Wolstencroft, R.D., Breon, F.-M. Polarization of Planet Earth and Model Earth-like Planets. In: *Astronomical Polarimetry: Current Status and Future Directions*. ASP Conference Series Vol. 343, 211-212 (2005).
- 16: Appenzeller, I., and 18 colleagues. Successful commissioning of FORS1 - the first optical instrument on the VLT. *The ESO Messenger* 94, 1-6 (1998).
- 17: MODIS web page <http://modis.gsfc.nasa.gov>
- 18: Palle, E., Zapatero Osorio, M.R., Barrena, R., Montanes-Rodriguez, P., Martin, E.L. Earth's transmission spectrum from lunar eclipse observations. *Nature* 459, 814-816 (2009).
- 19: Fox, G.K., Code, A.D., Anderson, C.M., Babler, B.L., Bjorkman, K.S., Johnson, J.J., Meade, M.R., Nordsieck, K.H., Weitenbeck, A.J., Zellner, N.E.B. Solar system observations by the Wisconsin Ultraviolet Photopolarimeter Experiment - III. The first ultraviolet linear spectropolarimetry of the Moon. *Mon. Not. R. Astron. Soc.* 298, 303-309 (1998).
- 20: Shkuratov, Y., Kaydash, V., Korokhin, V., Velikodsky, Y., Opanasenko, N., Videen, G. *Planetary and Space Science*, 59, 1326-1371 (2011).
- 21: Goloub, P., Deuze, J.L., Herman, M., Fouquart, Y. Analysis of the POLDER Polarization Measurements performed Over Cloud Covers. *IEEE Transactions on Geoscience and remote sensing*, Vol. 32, No. 1, 78-88 (1994).

22: Karalidi, T., Stam, D.M., Hovenier, J.W. Flux and polarisation spectra of water clouds on exoplanets. *Astron. Astrophys.* 530, A69 (2011).

23: Kokhanovsky, A., Platnick, S., King, M.D. Remote Sensing of Terrestrial Clouds from Space using Backscattering and Thermal Emission Techniques. In: *The Remote Sensing of Tropospheric Composition from Space*. Springer, Heidelberg. 231-257 (2011).

24: Tinetti, G., Meadows, V.S., Crisp, D., Kiang, N.Y., Kahn, B.H., Fishbein, E., Velusamy, T., Turnbull, M. Detectability of Planetary Characteristics in Disk-Averaged Spectra II: Synthetic Spectra and Light-Curves of Earth. *Astrobiology* 6, 881-900. (2006).

## Acknowledgement

Based on data collected with the Very Large Telescope under ESO-program 87.C-0040(A). EP acknowledges support from the spanish MICIIN grant #CGL2009-10641.

## Author contributions

MFS: Principal Investigator of the program. Observation preparation and execution. Data analysis and interpretation. Comparison with models. Writing of the manuscript.

SB: Co-Investigator. Observation preparation and execution. Data reduction and interpretation. Error analysis. Comparison with models. Contributions to the manuscript.

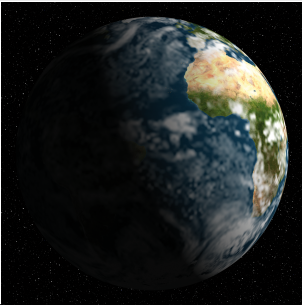
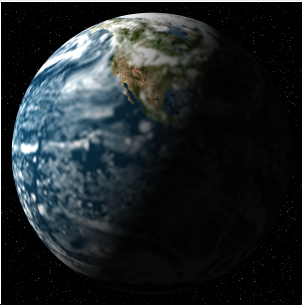
EP: Co-Investigator. Observation preparation. Data interpretation. Derivations of actual Earth surface fractions during the observations.

## Author information

Correspondence and requests for materials should be addressed to [msterzik@eso.org](mailto:msterzik@eso.org)

No competing financial interests exist.

**Table 1: Earth observations**

Observing Date	25-Apr-2011:UT09	10-Jun-2011:UT01
View of Earth as seen from the Moon		
Sun-Earth-Moon phase	87 deg	102 deg
ocean fraction in ES	18%	46%
vegetation fraction in ES	7%	3%
tundra, shrub, ice and desert fraction in ES	3%	1%
total cloud fraction in ES	72%	50%
cloud fraction $\tau > 6$	42%	27%

**Table 2: Model parameters**

Model	Ocean Clouded	Ocean Clear	Vegetation Clouded	Vegetation Clear	Line
April-a	48%	40%	0%	12%	————
April-b	60%	30%	10%	0%	- - - -
April-c	44%	56%	0%	0%	• • • • •
June-a	40%	60%	0%	0%	————
June-b	30%	60%	0%	10%	- - - -
June-c	27%	73%	0%	0%	• • • • •

### Table legend 1

*The detailed distribution of different types of surface contributions to the Earthshine. It has been determined by mapping satellite cloud retrievals from MODIS on the parts of the Earth's surface that are visible from the Moon at the given observing epoch<sup>17</sup>. The first observing epoch was before dawn on April 25 2011, and the Earthshine contains contributions from the Atlantic sea, the Amazonas region, and parts of Europe and Africa. The second observing epoch was after dusk on June 9 2011, and probes the Pacific side of the Earth, with almost no visible land surfaces. The contribution to the earthshine signal of a given Earth region will depend on the solar and lunar zenith angles (the reflectance is a bi-directional property), thus the percentage scene types and cloud cover fractions in the Table have been averaged over the whole earthshine-contributing area using these weights<sup>13</sup>. The contributions of clear tundra, shrub, desert or ice scenes were negligible.*

### Table legend 2

*Fractions of different types of surfaces used to model polarization spectra published in tables<sup>5</sup>. Parameters for "a" and "b" models are guided by observed scene type fractions in Table 1. The "c" models are generated through a grid of synthetic spectra and fit the observations best within 420 and 530nm. Note that the "Ocean Clouded" fractions agree well with the observed cloud fractions for optical depths  $\tau > 6$  in Table 1.*

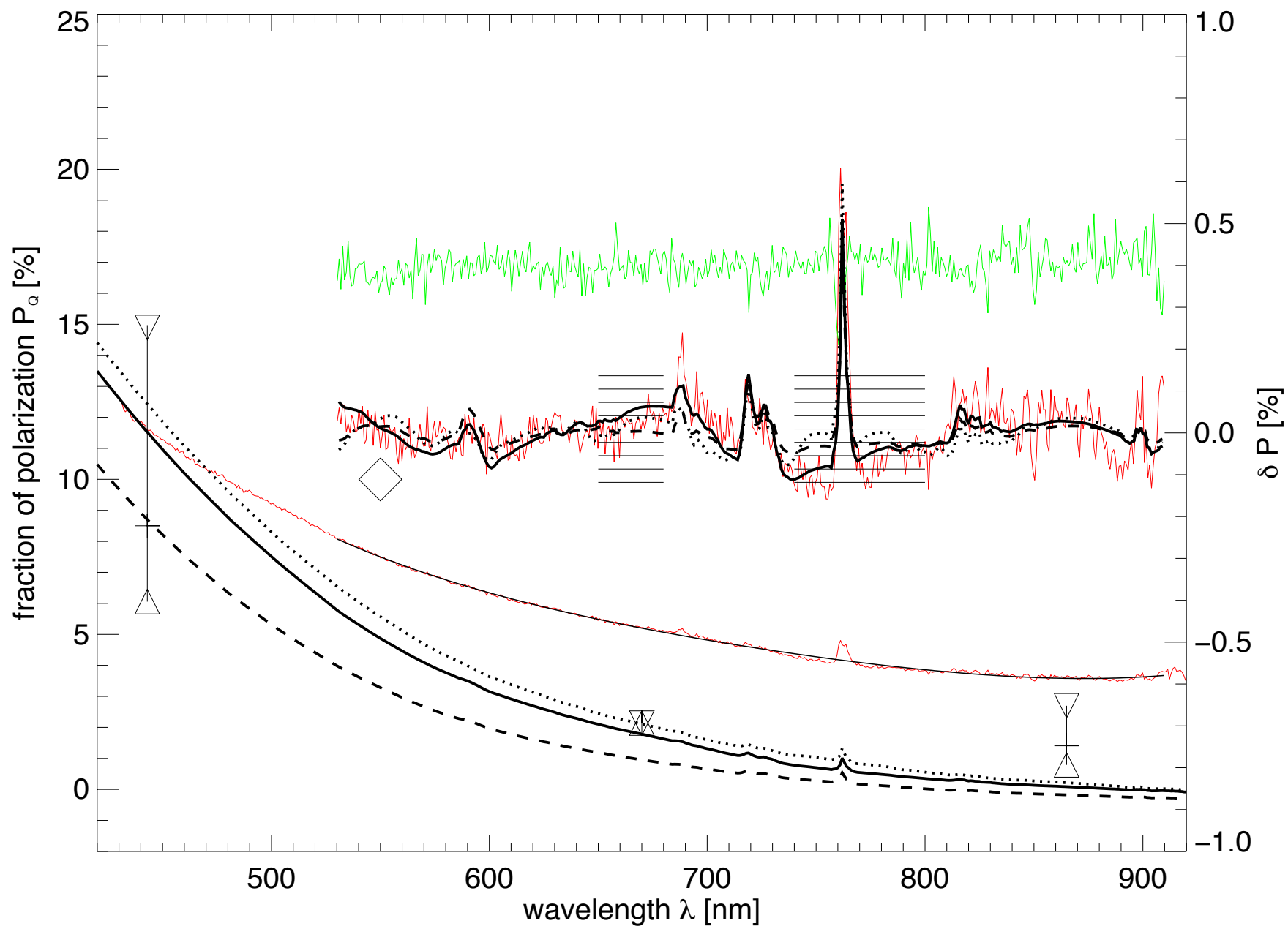


### Figure caption 1: Polarization spectra for April

*Polarization spectra observed in April showing the fractional polarization  $P_Q$  (red lines) and model comparison (black lines). For direct comparison with the Earthshine, the model spectra have been reduced in amplitude to account for the depolarization caused by the lunar surface<sup>19,20</sup>. The different linestyles refer to different choices of the model parameters, given in Table 2. The scale-units of the continuum polarization are shown on the left axis. The scale-units for the residuals are given on the right axis. The green line refers to measured  $P_U$  (same scale as the residuals on the right axis), and is representative for the noise level in the spectra. Vertically stacked lines between 650-680nm and 740-800nm denote the NDVI bandpass regions. POLDER-based whole-Earth polarization estimates are indicated at 443nm, 670nm and 865nm with a mean cloud coverage of 55%. Upper and lower triangles bracket low (10%) or high (90%) cloud coverage levels. Dollfus's estimate of an ES polarization of 10% at phase angle of 80 deg at 550nm is indicated by a diamond shaped symbol. A NDVI contrast is visible in the data and for model "a", which is consistent with a 10-15% visible vegetation content in the Earthshine.*

### Figure caption 2: Polarization spectra for June

*Polarization spectra observed in June. Explanations for the lines and symbols are the same as for Figure caption 1. A NDVI contrast is not evident in the data, and models "a" and "c" are consistent with no visible vegetation content in the Earthshine.*

